

# REPORT DOCUMENTATION PAGE

Form Approved  
OMB No. 0704-0188

Public reporting burden for this collection of information is estimated to average 1 hour per response, including the time for reviewing instructions, searching existing data sources, gathering and maintaining the data needed, and completing and reviewing the collection of information. Send comments regarding this burden estimate or any other aspect of this collection of information, including suggestions for reducing this burden, to Washington Headquarters Services, Directorate for Information Operations and Reports, 1215 Jefferson Davis Highway, Suite 1204, Arlington, VA 22202-4302, and to the Office of Management and Budget, Paperwork Reduction Project (0704-0188), Washington, DC 20503.

1. AGENCY USE ONLY (Leave blank) 2. REPORT DATE January 1994 3. REPORT TYPE AND DATES COVERED Final, 1 Sep 91 - 31 Aug 93

4. TITLE AND SUBTITLE Thermodynamics and Statistical Mechanics of Vibrations of Beams 5. FUNDING NUMBERS F49620-91-C-0074

6. AUTHOR(S) V. Berdichevsky and S Hanagud

7. PERFORMING ORGANIZATION NAME(S) AND ADDRESS(ES) Department of Mechanical Engineering Georgia Institute of Technology Atlanta, GA 30332

AFOSR-TR-97

0019

9. SPONSORING / MONITORING AGENCY NAME(S) AND ADDRESS(ES) AFOSR 110 Duncan Avenue, Suite B115 Bolling AFB, DC 20332 10. SPONSORING / MONITORING AGENCY REPORT NUMBER

NA

11. SUPPLEMENTARY NOTES

12a. DISTRIBUTION AVAILABILITY STATEMENT Approved for Public Release; Distribution Unlimited 12b. DISTRIBUTION CODE

13. ABSTRACT The primary goal of this research is to investigate whether the laws of statistical mechanics can be applied to structural vibrations. To achieve a qualitative understanding of the situation, investigation has been pursued on issues: deviation from equipartition, energy thresholds, energy transfer from low to high frequency modes, energy transfer from high to low frequency modes, correlation radius and geometry of phase space. Issues on dissipative systems, high energy vibrations, and "Planck Constant" for structural beams have also been investigated. From this research, it is found that there exists a sequence of energy thresholds for beam vibrations. They characterize the energy levels which should be exceeded in order to get equipartition of kinetic energy over the beam particles. The maximum energy threshold corresponds to the transition to developed chaos. Computational simulations indicate that upper energy threshold decays at low number of degrees of freedom and seems to grow at large number of degrees of freedom. The work also leads to the development of thermodynamics of limit cycles which has been applied to Duffing's oscillator and cantilever beam.

14. SUBJECT TERMS Energy Thresholds, Statistical Mechanics, Structural dynamics Modes Thermodynamics 15. NUMBER OF PAGES 28 16. PRICE CODE

17. SECURITY CLASSIFICATION OF REPORT Unclassified 18. SECURITY CLASSIFICATION OF THIS PAGE Unclassified 19. SECURITY CLASSIFICATION OF ABSTRACT Unclassified 20. LIMITATION OF ABSTRACT Unclassified

19970117 088

DTIC QUALITY INSPECTED 1

Standard Form 298 (Rev. 2-89)

## Thermodynamics and Statistical Mechanics of Vibrations of Beams

### Participating Students:

October 1992-December 1992:

Akif Özbek (nonsupported)

Won-Wook Kim(nonsupported)

January 1993-August 1993:

Akif Özbek (supported)

Igor Shekhtman (supported)

Advisor: Victor Berdichevsky

## Contents

1	Overview	2
2	Longitudinal Vibrations of Elastic Beams	5
3	A Qualitative Picture of Nonlinear Vibrations	8
3.1	Deviation from Equipartition . . . . .	8
3.2	Energy Thresholds . . . . .	11
3.3	Energy Transfer from Low Frequency Modes to High Frequency Modes	12
3.4	Energy Transfer from High Frequency Modes to Low Frequency Modes	13
3.5	Correlation Radius . . . . .	13
3.6	Geometry of Phase Space . . . . .	16
4	Is There a "Planck Constant" for Vibrations of Beams?	17
5	High Energy Vibrations of a Cantilever Beam	18
6	Dissipative Systems	19
7	Major Accomplishments	19
8	Publications and Presentations	20

# 1 Overview

The driving idea of this research is that there are some general relationships among dynamical characteristics of vibrating systems. We arrive at this idea when we compare the systems studied in statistical mechanics and structural mechanics. One of the favorite systems of statistical mechanics is a set of mass particles connected by springs (Fig. 1). We obtain the same kind of systems if we discretize the equations of elastic structures. For example, discretization of the dynamical equations of beams leads to a chain of mass particles (Fig. 2), while for more complex structures one obtains configurations in space like the one shown in Fig. 3.

Another example of the similarity is black body radiation: dynamical equilibrium of an electromagnetic field in a closed region (symbolically shown in Fig. 4). Electromagnetic field is described by linear Maxwell equations. It interacts with the charges on the wall in a nonlinear way. There is a very close structural analogy to this problem: a linear elastic beam connected to two nonlinear springs. The linear beam is described by linear wave equation (which mimics Maxwell equations).

It seems natural to assume that the laws of statistical mechanics might be valid for structural vibrations

There is, however, an important difference between the ensembles of oscillators in statistical mechanics and structural oscillators. In structures we often have to take into account friction, while in statistical mechanics oscillators are nondissipative. We will return to this point in Section 6, and now let us focus only on the elastic nondissipative free structural vibrations.

The first attempt to apply statistical mechanics to a chain of oscillators was undertaken about 40 years ago by E. Fermi, J. Pasta, and S. Ulam [1]. In terms of beam vibrations, they considered a discretized version of the equation for nonlinear longitudinal vibrations of an elastic beam with the stress-strain relation of the form

$$\sigma = E_Y(\varepsilon + \beta\varepsilon^3) \quad (1)$$

where  $\sigma$ ,  $E_Y$ ,  $\varepsilon$ , and  $\beta$  are stress, Young's modulus, strain and nonlinearity parameter, respectively. The displacements  $u(x, t)$  obey the equation

$$\frac{\partial^2 u}{\partial t^2} = \frac{\partial}{\partial x} \left( \frac{\partial u}{\partial x} + \beta \frac{\partial u^3}{\partial x} \right) \quad (2)$$

where  $t$  is time  $\cdot (\frac{E_Y}{\rho})^{\frac{1}{2}}$ , and  $\rho$  is density of the beam.

It was a common belief that the laws of statistical mechanics are valid for systems with a very large number of degrees of freedom. Since a 1-D continuum possesses an infinite number of degrees of freedom, one may expect that the laws of statistical mechanics can be applied to solutions of equation (2). To study the behavior of these solutions, equation (2) was replaced by a finite difference equation. The simplest test for validity of statistical relations is the equipartition of energy. If  $u_i$  is the displacement of the  $i$ th node, then the equipartition of energy means

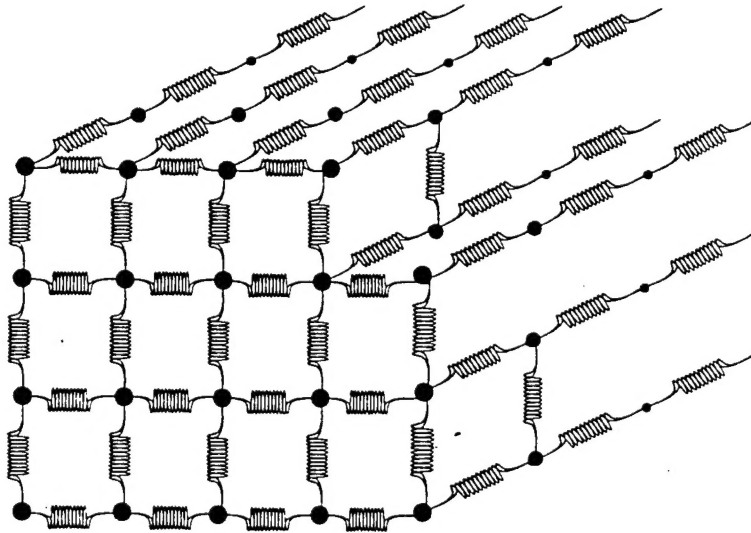


Figure 1: An Ensemble of Particles Connected by Springs



Figure 2: A Chain of Particles Connected by Springs

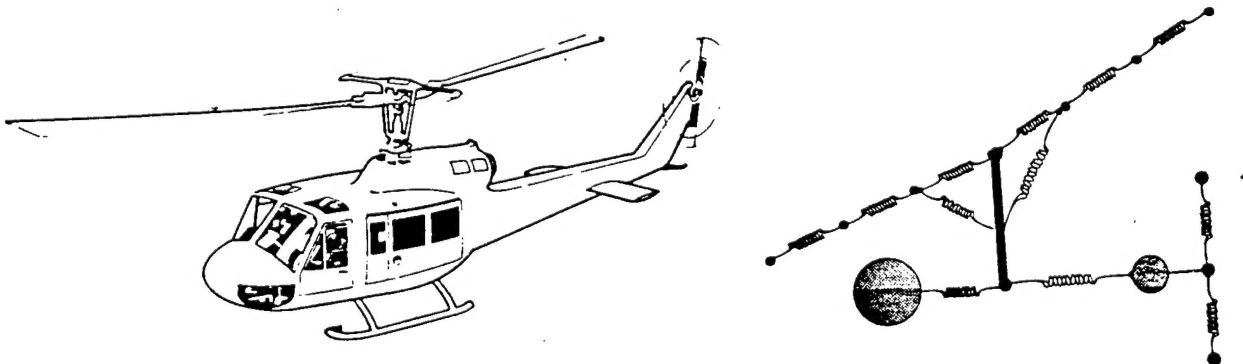


Figure 3: A Helicopter and Its Model

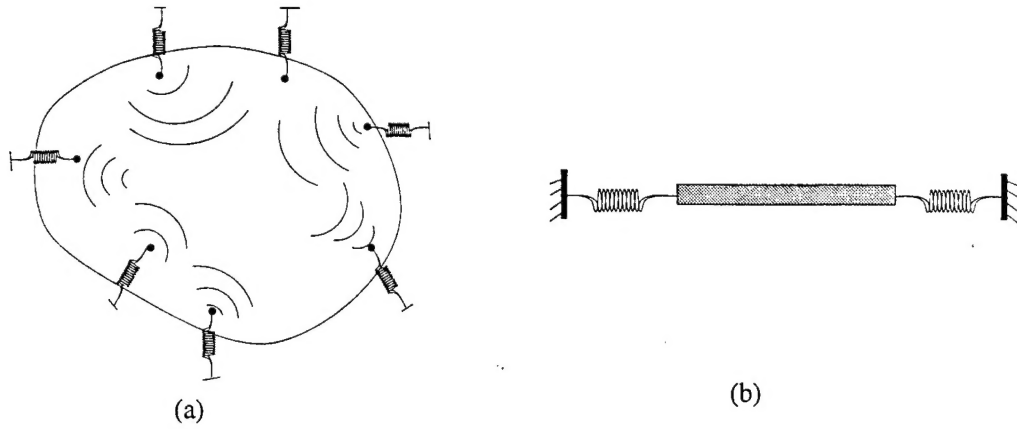


Figure 4: (a) Black Body Radiation. (b) Related Structural Problem: Linear Beam linking Two Nonlinear Springs

$$\langle m \dot{u}_1^2 \rangle = \langle m \dot{u}_2^2 \rangle = \dots = \langle m \dot{u}_n^2 \rangle \quad (3)$$

where  $m$  is the node mass, and  $\langle \cdot \rangle$  denotes the time average along a trajectory: for any function  $\rho(u_i, \dot{u}_i)$

$$\langle \rho(u_i, \dot{u}_i) \rangle = \lim_{\theta \rightarrow \infty} \frac{1}{\theta} \int_0^\theta \rho(u_i(t), \dot{u}_i(t)) dt \quad (4)$$

For systems considered in statistical mechanics (ergodic systems) motion is chaotic and the average values do not depend on the initial data. The common value (3) is called, by definition, temperature  $T$ . Equipartition of energy is a necessary condition for the laws of statistical mechanics to be true.

The discretized equation (2) was studied numerically [1] for the number of points in the  $x$ -direction,  $N$ , equal to 64. Surprisingly, it turned out that equipartition does not hold while the system exhibits a recurrent motion. The situation was cleared up to some extent by KAM theory [2]. According to KAM theory, for low excitation energies, the beam vibrates approximately as a linear body, and there is no equipartition of energy over the degrees of freedom. This is exactly what has been observed in numerical experiments by Fermi, Pasta and Ulam, where excitation energy was relatively small. KAM theory tells nothing about large energy excitation. In this case only numerical results have been obtained so far.

Unfortunately, in the papers published on this subject, one comes across many contradictory statements. Putting aside the detailed discussion of the results reported previously (this will be done in a publication), herein the picture emerging from our numerical simulations is described. One detail of this picture—the existence of upper energy threshold—can be found in previous publications [3]–[7], but the entire picture is presented here for the first time.

## 2 Longitudinal Vibrations of Elastic Beams

At present the only way to establish the applicability of statistical mechanics to structural vibrations is to conduct numerical or laboratory experiments. Computer experiments have been preferred for this study because they provide very easy parametric control. Since our goal is to achieve a qualitative understanding of the situation, we have to choose a structural model which, on one hand, is as simple as possible, and on the other hand, captures the main features of nonlinear vibrations. Longitudinal vibrations seem ideal for these purposes.

Longitudinal vibrations are characterized by one kinematical field: the longitudinal displacement  $u(x, t)$ . Lagrangian of longitudinal vibrations has the form

$$L = A\left(\frac{1}{2}\rho u_t^2 - U(\varepsilon)\right) \quad (5)$$

where  $u_t = \frac{\partial u}{\partial t}$ ,  $\varepsilon = \frac{\partial u}{\partial x}$ , and  $A$  is the area of the beam cross-section. Coordinate  $x$  is considered as the Lagrangian coordinate of beam particles. Energy density  $U(\varepsilon)$  is assumed to be a convex function of strain  $\varepsilon$ . The corresponding dynamical equation of free vibrations is

$$\rho \frac{\partial^2 u}{\partial t^2} = \frac{\partial}{\partial x} \frac{\partial U(u_x)}{\partial u_x} \quad (6)$$

For the Fermi-Pasta-Ulam (FPU) problem

$$U = \frac{1}{2}E_V(\varepsilon^2 + \frac{1}{2}\beta\varepsilon^4) \quad (7)$$

Expression for energy density (7) can only be used for moderate strain  $\varepsilon$ , because  $U$  should have a singularity at the strain value  $\varepsilon = -1$ . This value corresponds to the collapse of the material segment to a point. The simplest model that satisfies the singularity condition is the Neo-Hookian material

$$U = \frac{\mu}{2}u_x^2 \frac{3 + u_x}{1 + u_x} \quad (8)$$

where  $\mu$  is the shear modulus for small strains. The model (8) describes the elastic properties of some rubbers quite well.

We performed numerical simulations for both cases (7) and (8). They look qualitatively similar, therefore all figures presented below are for the FPU model. The only exception is Section 5, where we evaluate the range of strains where our conclusions are valid for rubbers.

To set up a finite dimensional model we discretize the continuum beam, and consider a chain of interacting "particles" (nodes) with the Lagrange function

$$L = \sum_{i=1}^N \left( \frac{1}{2}u_i^2 - U(\varepsilon_i) \right) a \quad (9)$$

where  $u_i$  is the displacement of the  $i$ th particle,  $a$  is the distance between neighboring particles, and  $\varepsilon_i = u_{i+1} - u_i/a$ ,  $a \cdot N = \ell$ .

We use periodic boundary conditions for our simulations. This means that  $u_{N+1} = u_1$ . In fact, our results do not depend on the choice of the boundary conditions, this will be explained in Section 5. Discretized version of the equation of motion is taken in the form

$$\frac{\partial L}{\partial u_i} - \frac{d}{dt} \frac{\partial L}{\partial \dot{u}_i} = 0 \quad (10)$$

The laws of statistical mechanics were derived at the so called thermodynamical limit. This means that number of particles and energy per unit volume are kept constant while the size of the system, the total energy and the total number of particles  $N$  tend to infinity. In our case this corresponds to fixed particle distance  $a$  and fixed energy per unit length, while the beam length  $\ell = aN$  and the total energy  $E$

$$E = \int_0^\ell \left( \frac{1}{2} \rho u_i^2 + U(\varepsilon) \right) dx \quad (11)$$

tend to infinity.

One might consider another limit, continuum limit, when the length of the beam  $\ell$  and total energy  $E$  are fixed, while the total number of particles  $N$  tends to infinity. In this case the distance between neighboring particles  $a = \ell/N$  tends to zero. In general, these two limits are different. However, longitudinal beam vibrations possesses the remarkable property that the thermodynamical limit coincides with the continuum limit. This can be seen if we scale time, axial coordinate, and displacement, and introduce dimensionless quantities

$$\tau = \frac{t}{\ell} \sqrt{\frac{E_Y}{\rho}}, \quad \xi = \frac{x}{\ell}, \quad v = \frac{u}{\ell} \quad (12)$$

where

$$E_Y = \lim_{\varepsilon \rightarrow 0} \frac{U(\varepsilon)}{\frac{1}{2} \varepsilon^2}$$

We can write

$$U(\varepsilon) = E_Y U_o(\varepsilon)$$

where  $U_o(\varepsilon)$  is the dimensionless energy density. The action functional of the system takes the form

$$\int_{t_1}^{t_2} L dt = \int_{\tau_1}^{\tau_2} A E_Y \ell L_o d\tau \quad L_o = \frac{1}{2} v_\tau^2 - U_o(v_\xi) \quad (13)$$

Since after scaling the action functional has the same form (up to a factor), the equation of motion also has the same form, and thermodynamical limit  $\ell = aN \rightarrow \infty$  is reduced after scaling to continuum limit on the unit segment  $0 \leq \xi \leq 1$ .



Note that the coincidence of the thermodynamical and continuum limits takes place only for longitudinal vibrations. These limits are different for lateral vibrations. This will be further explained in Section 6.

For definiteness the following will be carried in in the continuum limit.

One useful note should be made here. In the case of the FPU model the scaled Lagrangian has the form

$$L_o = \frac{1}{2}v_\tau^2 - \frac{1}{2}(v_\xi^2 + \frac{1}{2}\beta v_\xi^4)$$

An additional scaling is possible which reduces the FPU Lagrangian to a standard form with  $\beta = 1$ . This scaling is

$$v \rightarrow w : \quad v = \frac{1}{\sqrt{\beta}}w, \quad \tau \rightarrow \lambda : \quad \tau = \sqrt{\beta}\lambda$$

we have

$$L_o = \frac{1}{\beta}[\frac{1}{2}w_\lambda^2 - \frac{1}{2}(w_\xi^2 + \frac{1}{2}w_\xi^4)]$$

Hence, after scaling, dynamical equations of the FPU model coincides with the original equation with  $\beta = 1$ . Therefore, all results are presented below for the case  $\beta = 1$ .

### 3 A Qualitative Picture of Nonlinear Vibrations

#### 3.1 Deviation from Equipartition

Our primary goal is to establish whether the laws of statistical mechanics can be applied to structural vibrations. To this end, we started from probes of equipartition of energy over degrees of freedom. We measured "partial temperatures"

$$T_i = \rho a \langle \dot{u}_i^2 \rangle \equiv \lim_{\theta \rightarrow \infty} \frac{1}{\theta} \int_0^\theta \rho a \dot{u}_i^2 dt \quad (14)$$

In reality, we measured the quantities

$$\frac{1}{\theta} \int_0^\theta \rho a \dot{u}_i^2 dt \quad (15)$$

and used that time of observation  $\theta$  can be taken not very large because the partial temperatures approach their limit values fairly fast. Typical dependence of quantities (15) on  $\theta$  is shown in Fig. 5. In all the graphs time refers to dimensionless time  $\tau$  (12). The largest dimensionless period of vibrations of a linear spring is of order unity. Usually time  $\theta = 1000$  is enough to reach the limit values of partial temperatures.

Deviation from equipartition can be measured by the quantity

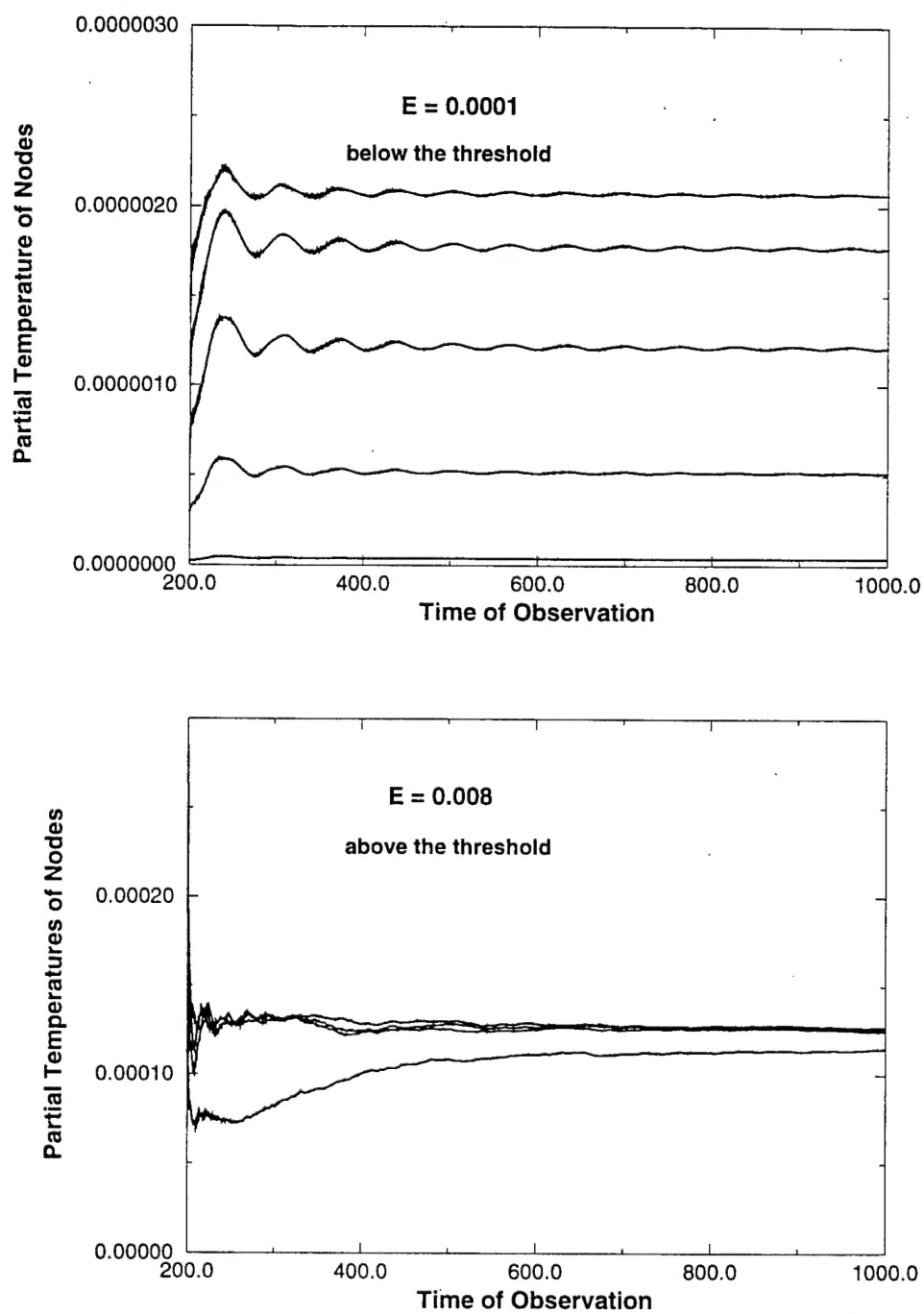


Figure 5: Dependence of Partial Temperatures on Time of Observation

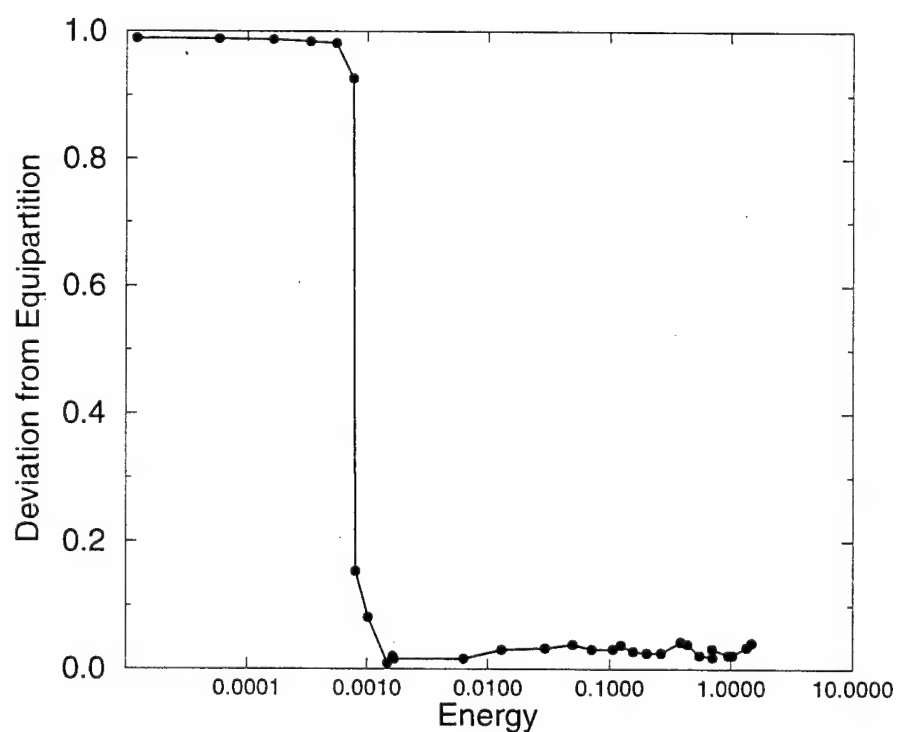
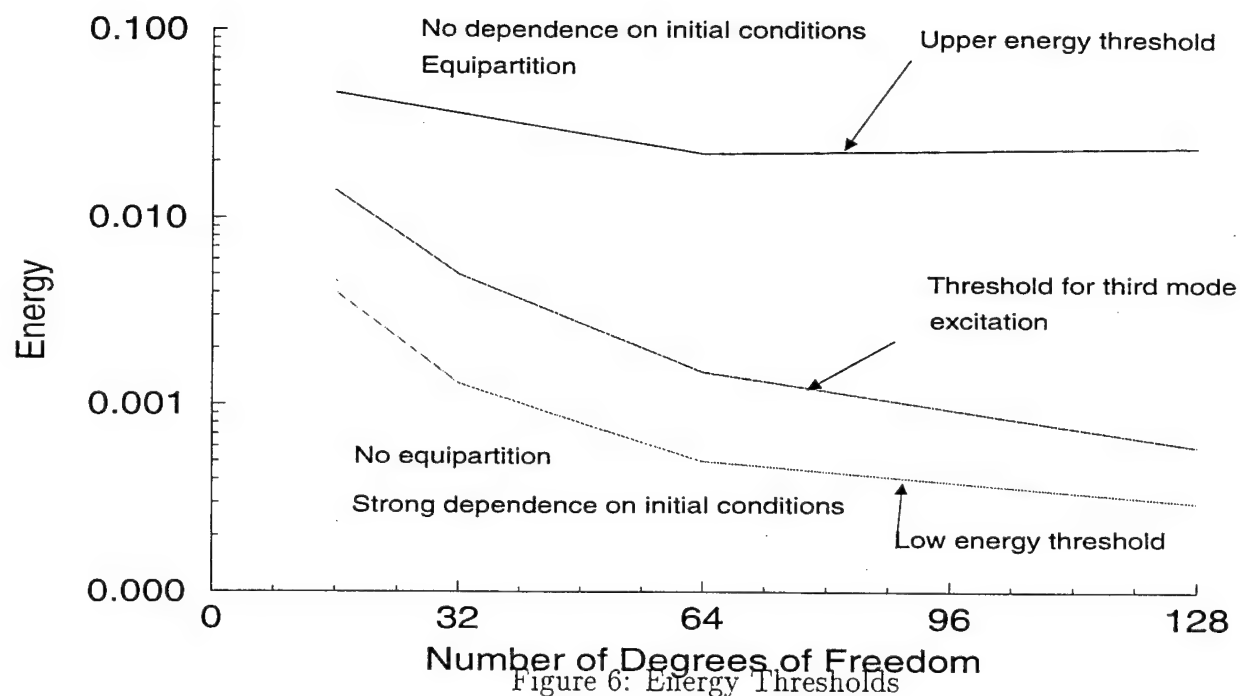


Figure 7: Deviation From Equipartition for First Mode Excitation

$$\Delta = \max\left\{\frac{T_1 - \bar{T}}{\bar{T}}, \dots, \frac{T_N - \bar{T}}{\bar{T}}\right\}$$

where  $\bar{T}$  is the temperature averaged over the nodes

$$\bar{T} = \frac{T_1 + T_2 + \dots + T_N}{N}$$

### 3.2 Energy Thresholds

We studied the dependence of  $\Delta$  on the energy of initial excitation. We revealed the existence of a number of characteristic values of energy, energy thresholds, exceeding of which is characterized by changes in beam dynamics. These thresholds are shown in Fig. 6. Now let's discuss what all the lines in this figure mean.

Let's consider an initial excitation of a single mode. In this case the initial data is taken in the form

$$\begin{aligned} v_i(0) &= q_i^k \sin \frac{2\pi i k}{N} + \tilde{q}_i^k \cos \frac{2\pi i k}{N} \\ \dot{v}_i(0) &= p_i^k \sin \frac{2\pi i k}{N} + \tilde{p}_i^k \cos \frac{2\pi i k}{N} \end{aligned} \quad (16)$$

where  $k$  is the mode number. Hence for each single mode of excitation we have 4 parameters which can be varied arbitrarily or 3 parameters if the energy value<sup>1</sup> is prescribed.

Let's first excite the lowest mode. If the energy of excitation is small, the final temperature distribution depends significantly on initial data. However, if we exceed some energy value, the first energy threshold, dependence on initial data disappears while energies are approximately equally distributed over the nodes. The dependence of  $\Delta$  on the energy of excitation can be seen in Fig. 7. There is a fairly sharp drop in  $\Delta$  for  $E^* \simeq 10^{-3}$ . Deviations from equipartition  $\Delta$  for  $E^* > 10^{-3}$  are not zero but small, in the order of 0.05.

In fact, we observe a narrow range of energies for which this drop occurs. Moreover, if we try many initial conditions for the first mode excitation, we get a distribution

---

<sup>1</sup>Energy shown in all the graphs is dimensionless energy  $E^*$ ,

$$E^* = \int_0^1 \left( \frac{1}{2} v_\tau^2 + U_o(v_\xi) \right) d\xi,$$

it relates to the "usual" energy  $E$  by the formula

$$E = \int_0^\ell \left( \frac{1}{2} \rho u_t^2 + U(u_x) \right) dx = A \ell E_Y E^*$$

of energy thresholds with a peak. For the sake of brevity, we will call it as “energy threshold”, and attach the corresponding characteristic value of energy.

Simulation show that the value of the energy threshold decays with the growth in the number of degrees of freedom. It seems very plausible that the first energy threshold reaches some asymptotic value when  $N \rightarrow \infty$ .

What happens if we initially excite a higher mode, say, the third one? The situation is very similar to the previous one with the only difference: energy threshold for the third mode is approximately 10 times higher than the first energy threshold. It seems that it also approaches some limit value.

For the even modes the behavior of the energy thresholds is different: energy threshold does not grow monotonically with energy growth. We assume that this degeneracy relates to the resonance existing between even modes due to the evenness of the number of degrees of freedom. This degeneracy should disappear when we consider systems with an odd number of degrees of freedom. This hypothesis has been checked for 17 degrees of freedom, and the simulations support it very well.

It turns out that there are two energy thresholds, low energy threshold,  $E_c$ , and upper energy threshold,  $E^c$ , such that for energy values below  $E_c$  motion is ordered, and for values above  $E^c$  motion is approximately ergodic, and equipartition holds. In the intermediate region the character of motion depends on which modes are excited. Low energy threshold is approximately equal to the first energy threshold.

Low energy threshold seems not to depend on  $N$  for large  $N$ , while upper energy threshold seems to grow with increasing  $N$  although for small  $N$  we observe decay of the upper energy threshold (see Fig. 6).

What happens if we excite, for example, the first three modes simultaneously? Of course the energy threshold is  $E_3$ . If all modes are involved in the initial excitation, then equipartition can only be guaranteed if the energy of excitation is greater than the upper energy threshold  $E^c$ .

Upper energy threshold was predicted by Chirikov and Israilev [5] and was observed for the first time by Bocchiery et. al. [3] for a chain with Lennard-Jones interaction. However there are conflicting statements about the behavior of upper energy threshold when  $N$  grows. For example, in [5, Kantz] energy thresholds decay for large  $N$ . As it was mentioned, our results support simulations by Bocchiery et.al[3].

### 3.3 Energy Transfer from Low Frequency Modes to High Frequency Modes

Let us now consider energy thresholds from the perspective of energy transfer between modes. Let only the first mode be excited. The energy spectra for various values of energy are shown on Fig. 8. Do not pay attention to the “teeth” on the curves, as they relate to the short time of averaging. When we do longer runs, these curves get smoother. We chose a time of averaging in such a way that we obtain results within

a reasonable amount of time.

For low energy excitation,  $E^* = 10^{-5}$ , which is far below  $E_c$ , energy is passed over the first four neighboring modes. When  $E^* = 10^{-4}$ , first 8 modes are involved in motion. In the vicinity of  $E_c$  (Fig. 8(e)), about half of the modes are excited. This seems peculiar, at the first glance, because equipartition of spatial distribution of temperature is observed at these values of energy. It is known from statistical mechanics, that, if equipartition holds in one set of coordinates, it also holds in any other set of coordinates. In our case these sets of coordinates are displacement at nodes and amplitudes of modes. The explanation relates to the tail of the curve in Fig. 7. Deviation from equipartition is small but not zero. This "allows" high modes, in Fig. 8, not to be excited. Further increase of energy initiates stronger energy flow, and, when energy exceeds the upper energy threshold, we observe equipartition over modes (Fig. 8(h)). Note a specific feature of energy transfer: decrease of energy leads to "freezing" high frequency modes.

### 3.4 Energy Transfer from High Frequency Modes to Low Frequency Modes

Transfer of energy from high modes to low modes (sometimes referred to as "backward energy flow", in contrast to "forward energy flow" in the case of energy transfer from low to higher modes) has some import peculiarities. To discuss them consider, for definiteness, initial excitation of the 5th mode. Energy spectra for various values of excitation energy<sup>2</sup> are shown in Fig. 9. It is instructive to compare Fig. 8 and Fig. 9. First of all, we see that for  $E^* = 10^{-5}$  only the fifth mode is excited (Fig. 9(a)) while the first mode transmits its energy to the three neighboring modes. For  $E^* = 10^{-4}$ , the resonance of fifth and tenth modes becomes visible and only these two modes are excited (Fig. 9(b)), while the first mode conveys its energy to the 8 neighboring modes. For  $E^* = 10^{-4}$ , the resonance of fifth and tenth modes become more pronounced while the energy of the first mode is transferred to the 12 neighboring modes. For  $E^* = 10^{-3}$  the new resonance of 15th mode becomes visible, but still only 3 modes are excited, while the first mode shares its energy with 15 other modes. We conclude that transfer of energy occurs very easily from low modes to high modes, and backward energy flow is impeded. Physically, it seems quite natural because high frequency oscillators are more stable and one needs to supply much more energy in order to provide the interactions with other oscillators. Impediment of backward energy flow disappears when the energy exceeds the upper energy threshold: energy can go back and forth without any obstacles.

<sup>2</sup>The same as for the first mode on Fig. 8.

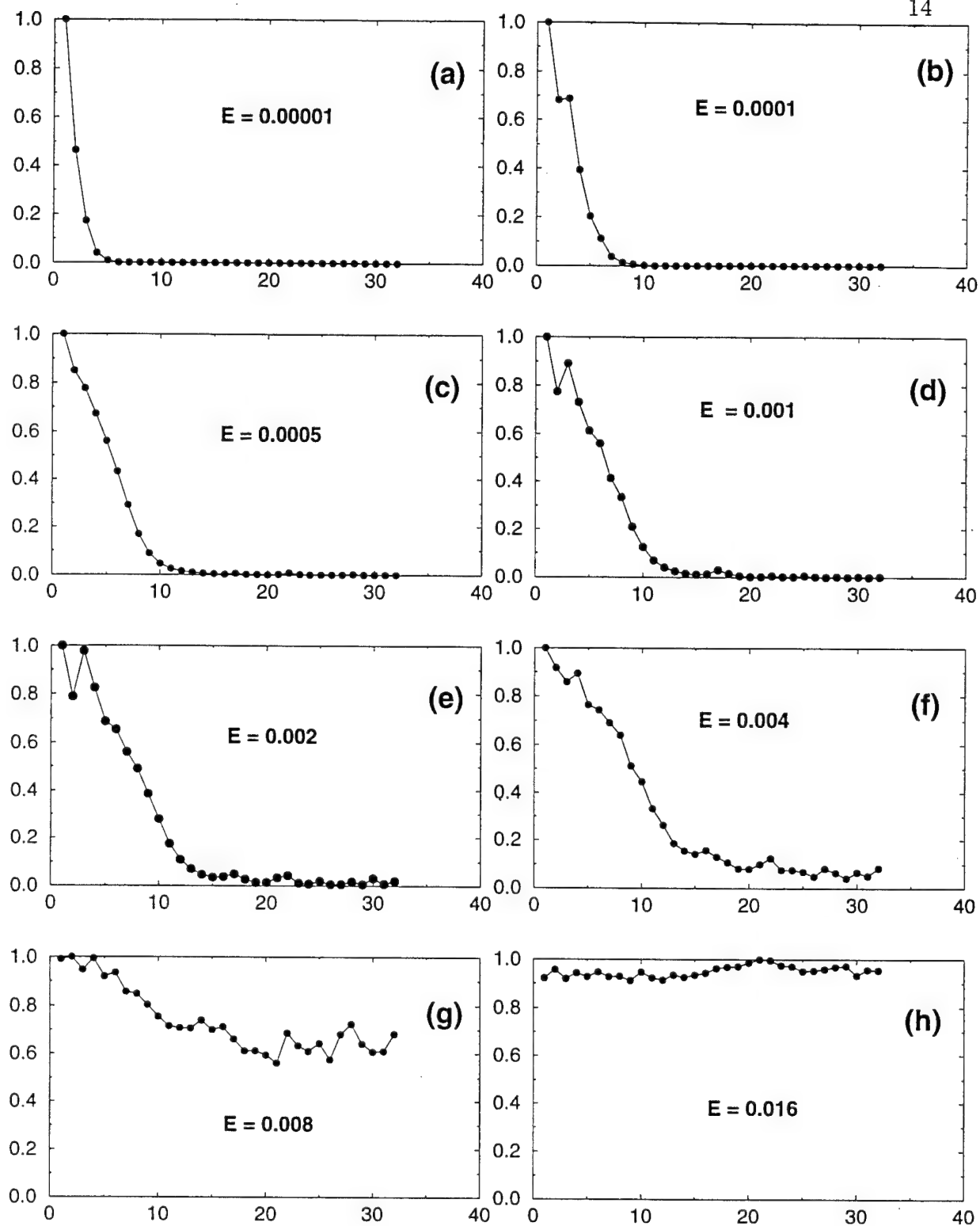


Figure 8: Energy Spectrum for First Mode Excitation

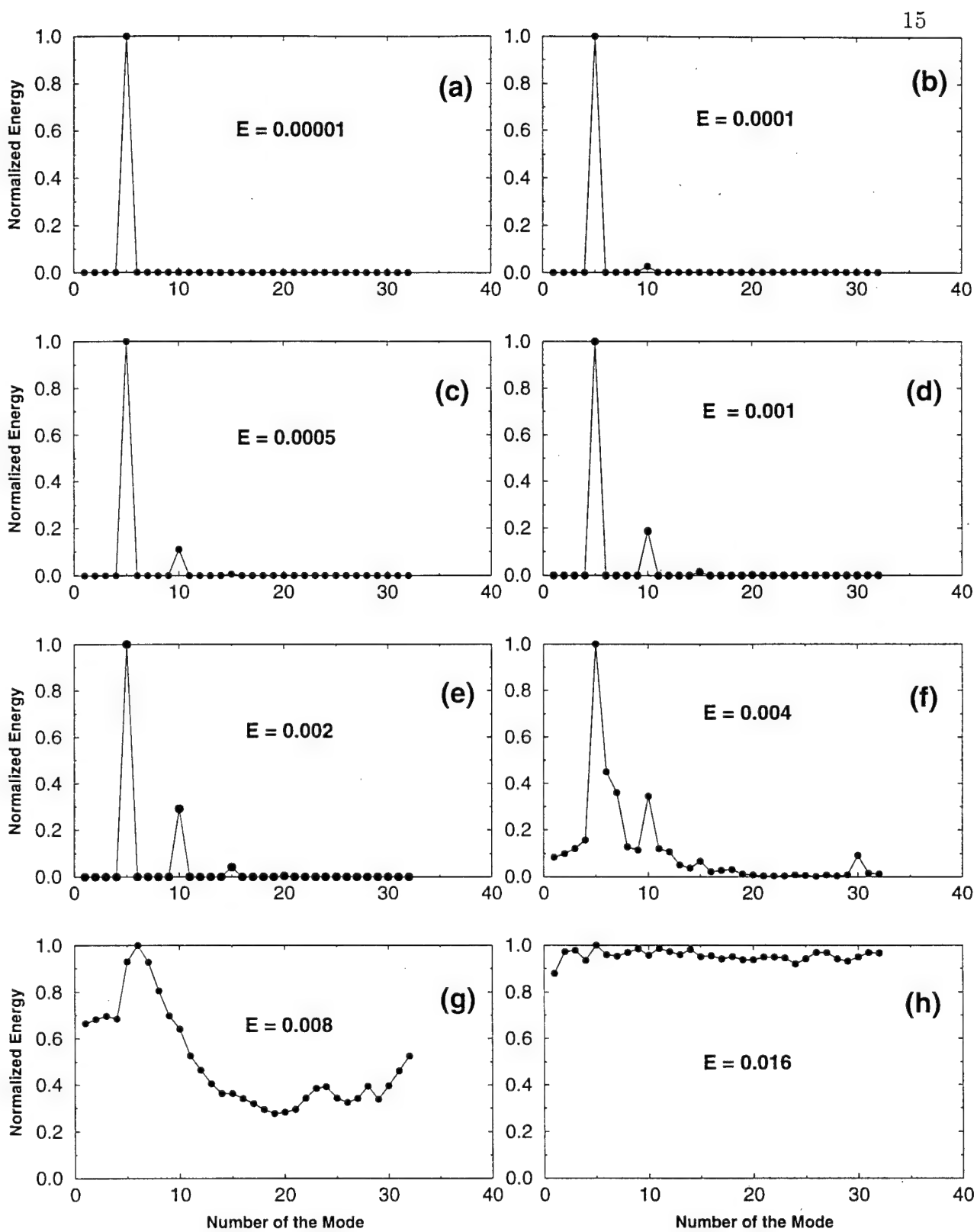


Figure 9: Energy Spectrum for Fifth Mode Excitation



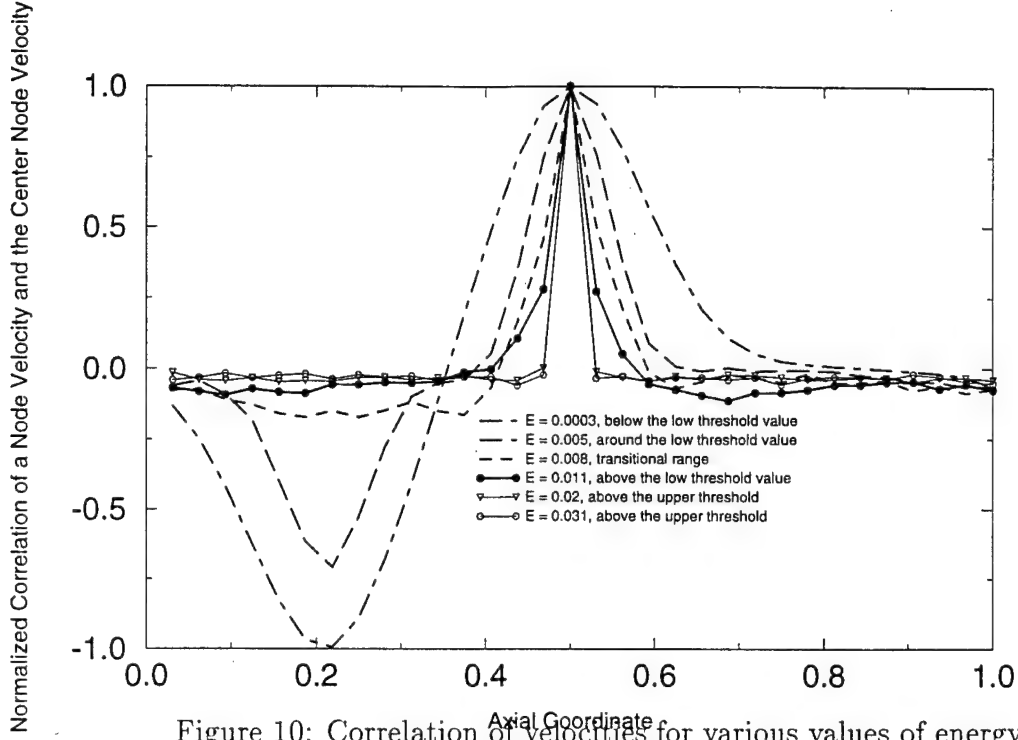


Figure 10: Correlation of velocities for various values of energy

### 3.5 Correlation Radius

In the preceding subsections we have seen that the motion is not completely chaotic at low energy threshold. Another confirmation of this observation comes from the study of the correlation radius. We measured velocity correlations  $\langle \dot{u}_i \dot{u}_j \rangle$  ( $i, j = 1, 2, \dots, N$ ) and considered their dependence on the distance between the nodes  $i - j$ . Typical graphs of this dependence are shown in Fig. 10. Here  $\langle \dot{u}_k \dot{u}_{16} \rangle / \langle \dot{u}_{16} \rangle$  is plotted as a function of the node number  $k$  for various values of energy of excitation of the first mode, and  $u_{16}$  is the displacement of the center of the 32 particle chain. When  $E^* = 0.003$ , which is below  $E_c$ , strong correlation is observed. Asymmetry relates to the dependence of correlations on initial conditions: the curve retains the asymmetry of the prescribed asymmetric initial data. Around the threshold, we see the nonzero correlation decays as energy is getting larger. When the upper energy threshold  $E^c$  is reached correlation practically disappears. This confirms that the motion for  $E > E^c$  is practically ergodic.

### 3.6 Geometry of Phase Space

Above discussion sheds some light on the geometrical structure of the phase portrait of beam vibrations. Unfortunately, in multidimensional space we do not have such powerful tools as Poincaré maps for low-dimensional systems. Therefore, we have to be content with a qualitative picture. The sketches trying to give an idea on transformations of phase portrait are presented in Fig. 11-13.

If the energy of excitation is less than  $E_c$ , then the energy surface is occupied by ordered motion (Fig. 11). For larger energies parts of the islands of ordered motion

decay and become chaotic “straits” (Fig. 12). Further increase of the energy leads to the decay of the “lowest mode island” (Fig. 13). Lowest mode island disappears when the energy exceeds the low energy threshold  $E_c$ . A chaotic sea occupies a considerable part of the energy surface. If we increase the energy more, the chaotic sea absorbs the second mode island of ordered motion and so on. Of course, some of the islands associated with modes, can disappear simultaneously, or in a “inproper order”, depending on the peculiarities of the system. The highest mode island in our simulations survives until the energy exceeds the upper energy threshold. Then the chaotic sea occupies the entire energy surface, except very small islands of ordered motion, and motion becomes practically chaotic.

## 4 Is There a “Planck Constant” for Vibrations of Beams?

Consider again the spectral distribution for energy of excitation lying within the interval  $[E_c, E^c]$ . If motion were ergodic, energy is equally distributed over the modes, and the energy spectrum is the straight horizontal line (Fig. 14(a)). The ordinate of this line is  $T$ , because all modes carry the energy  $T$  due to equipartition.

In reality, we observe spectrum distribution shown in Fig. 14(b). This indicates that motion is not ergodic. We see that high modes are practically not excited, they are “frozen.” If we decrease energy further, more of the modes become frozen. This is very reminiscent of the difficulties which appeared in theoretical predictions of heat capacity of gases and black body radiation at low and high temperatures 100 years ago.

A theoretical formula for a spectrum distribution based on ergodic hypothesis and equipartition was suggested by Rayleigh and Jeans. In the 1D case it is exactly a straight line as shown in Fig. 14(a). In fact, Rayleigh and Jeans considered the 3D case, where spectrum is parabolic because the number of modes in an interval  $[\omega, \omega + d\omega]$  is proportional to  $\omega^2$ . Experiment confirmed the Rayleigh-Jeans formula for low frequencies, but revealed strong deviations for high frequencies. Qualitatively, the Rayleigh-Jeans spectrum and experimental spectrum are shown in Fig. 15.

Thinking about this contradiction, Jeans noticed that high frequency motion behaves as if it were frozen when we lower the temperature (or energy).

In 1900, Planck found a simple formula for spectrum distribution which fits very well with the experimental data. If we rewrite this formula for 1D vibration, it takes the form

$$E(\omega) = \frac{h\omega}{e^{\frac{h\omega}{T}} - 1} \quad (17)$$

where  $h$  is a constant determined from fitting to experimental data.

For low modes,  $T \gg h\omega$ , the exponent in (17) can be expanded in a Taylor series, and we obtain equipartition

$$E(\omega) = T$$

For high modes,  $h\omega \gg T$ , we have exponential decay of spectrum

$$E(\omega) = h\omega e^{-\frac{h\omega}{T}}$$

The form of Planck's spectrum is shown qualitatively in Fig. 16.

Later on, Planck invented the ergodic statistics of oscillators which leads to the energy spectrum (17). The statistics were based on quantum hypothesis, which in turn gave rise to quantum mechanics.

Comparing the curves of Fig. 8 and Fig. 16, we see a remarkable qualitative coincidence. Moreover, the underlying physics seem familiar: high frequency modes freeze if we lower energy. This suggests a number of ideas:

1. Try to fit experimental data for beam vibrations using Planck's distribution and check whether the Planck constant is a universal one for vibrations of beams.
2. Check to what extent Planck's statistics is applicable to beam vibrations.
3. We know that the dynamical origin of the spectrum decay is nonergodicity of motion. Maybe, there is an explanation of behavior of the quantum oscillator based on classical mechanics and nonergodicity without the quantum hypothesis?
4. Similarity of beam spectrum and quantum oscillator spectrum suggests that some correspondence might exist between statistical mechanics of nonergodic systems and quantum statistics.

At present, we are far from understanding all of that. Trying to get some insight, we started from an attempt to fit experimental data for a beam energy spectrum using Planck's formula (17). A typical fit is shown in Fig. 17. The Planck constant for beam vibrations can be presented in the form

$$h = Mc\ell\hat{h} \quad (18)$$

where  $M$ ,  $c$ , and  $\hat{h}$  are the mass of beam, speed of sound, and a dimensionless constant, respectively. The approximate value of  $\hat{h}$  is

$$\hat{h} = 0.003 \quad (19)$$

We are not in a position to claim that  $\hat{h}$  is a universal constant, universal in the sense that it is only material dependent. To establish that, we have to conduct a two-parametric study with respect to energy of excitation and the number of degrees of freedom. We have not done this yet because the idea of using Planck's spectrum came only recently. At present, we may say with some confidence that the value (19) does not depend on the number of degrees of freedom. A comprehensive study is now underway.

## 5 High Energy Vibrations of a Cantilever Beam

Now we are going to give some additional support to the idea that statistical mechanics is sensible for structural vibrations.

Consider free vibrations of a cantilever beam. Let us excite the lowest mode. Which temperature distribution shall we get? Temperature at the clamped edge should be zero; temperature at the free edge should be maximal. Our intuition, developed on linear vibrations, suggests the curve shown in Fig. 18.

But this is in obvious contradiction to equipartition! Therefore, either our intuition fails, or statistical mechanics does not work. What do the experiments show?

If energy of excitation is small, we observe a temperature distribution which really looks like the curve in Fig. 18. For  $E = 10^{-3}$  it is shown in Fig. 19. Note that motion is not ergodic for this value of energy. If we increase the energy level then temperature distribution changes; for  $E = 10^{-2}$  it is shown in Fig. 20. If we keep increasing energy and overcome the low energy threshold, temperatures become constant and we get practically ideal equipartition (Fig. 21).

It can be seen in Fig. 22 how temperature distribution approaches to equilibrium distribution; three curves correspond to successive moments of observation.

Again, for a cantilever beam we found the same energy thresholds as above: if the first mode is excited, transition to equipartition occurs at the first energy threshold; if the second mode is excited, then for equipartition energy should exceed the second energy threshold, and so on. Final temperature distribution does not depend on initial excitation if  $E > E^c$ .

Another conclusion which can be drawn out of these simulations is the independence of the equilibrium state from boundary conditions. It is seen that the edge zone does not penetrate into the interior portion of the beam. This is why our results for periodic boundary conditions are, in fact, universal.

The simulations have been conducted for both FPU and Neo-Hookean models. For Neo-Hookean material we found that the low energy threshold corresponds to the strains of order 0.2 – 0.3. This is a working regime for many rubbers and polymer materials.

## 6 Dissipative Systems

Thermodynamics and statistical mechanics of dissipative system of oscillators is an open field now, and only a few statements (like the existence of attractors) can be made. An attempt to extend thermodynamics to limit cycles was undertaken in papers [12] [13] [14]. The major results are:

1. Entropy disappears from thermodynamical relations because, after the transitional period, vibrations do not depend on initial data.(initial data enters in thermodynamical relations by means of entropy

2. The averaged Lagrangian takes place of energy in thermodynamical relations.

The general theory [10] has been considered for the examples of Duffing's Oscillator [13] and cantilever beam [14].

## 7 Major Accomplishments

1. It is established that there exists a sequence of energy thresholds for beam vibrations. They characterize the energy levels which should be exceeded in order to get equipartition of kinetic energy over the beam particles. The corresponding energy level depends on the wave length of initial excitation. The lowest energy threshold  $E_c$  corresponds to the first mode excitation. Second energy threshold  $E_2$  corresponds to the second mode excitation, and so on. For a beam model with  $N$  particles there are  $\frac{N}{2}$  energy thresholds. The maximum energy threshold (upper energy threshold  $E^c$ ) corresponds to the transition to developed chaos. For  $E > E^c$  the beam motion can be described by the relations of statistical mechanics. For  $E < E_c$  the beam motion is mostly ordered. In the intermediate region  $E_c < E < E^c$  motion of the beam is "partially chaotic" in the sense that energy exchange between beam particles is enough to reach equipartition but not enough to develop a completely ergodic motion.
2. The existence of upper energy threshold has been established previously in a number of publications, however, there are contradictory statements on the dependence of upper energy threshold on the number of degrees of freedom. Our simulations show that upper energy threshold decays at low number of degrees of freedom and seems to grow at large number of degrees of freedom.
3. The energy transfer has been studied in the energy range  $E_c > E > E^c$ . It was observed that energy is easily transferred from the low modes to higher modes but the backward energy flow (from high modes to low ones) is impeded. Analytically the energy transfer might be characterized by the energy spectrum which seems to be very well fitted by the Planck spectrum.
4. In computer simulations, the approach to the state with homogeneous distribution of temperature has been clearly observed for vibrations of a cantilever beam at high energies.
5. Thermodynamics of limit cycles has been developed and applied to Duffing's oscillator and cantilever beam

## 8 Publications and Presentations

*Publications:*

1. Berdichevsky, V., "Reciprocal Relations in Nonlinear Vibrations," *International Journal of Engineering Science*, Vol. 31, No. 8. pp. 1215-1218, 1993
2. Berdichevsky, V., "Generalized Equipartition Law," *International Journal of Engineering Science*, Vol. 31, No. 4. pp. 673-677, 1993.
3. Berdichevsky, V., Özbek, A., and Kim, W. W., "Thermodynamics of Duffing's Oscillator," *Journal of Applied Mechanics*, (to appear)
4. Berdichevsky, V., Kim, W. W., and Özbek, A., "Dynamical Potential for Nonlinear Vibrations of a Cantilever Beam," *Journal of Sound and Vibrations*, (to appear)
5. Berdichevsky, V. "Thermodynamics of Chaos", Pittman-Longman (to appear) 1994

*Presentations:*

1. Berdichevsky, V., Özbek, A., "Statistical Mechanics of the Duffing Oscillator", presented at Dynamics Days Texas, January 8-11, 1992.
2. Özbek, A., and Berdichevsky, V., "Thermodynamics of Duffing's Oscillator," presented at SIAM Conference on Applications of Dynamical Systems, Salt Lake City, Utah, October 15-19, 1992.
3. Berdichevsky, V., "Thermodynamics of Chaotic Vibrations," presented at SIAM Conference on Applications of Dynamical Systems, Salt Lake City, Utah, October 15-19, 1992.
4. Berdichevsky, V. "Statistical Mechanics of Structural Vibrations," presented at the Symposium and Workshop on Nonlinear Dynamics of Aerospace Structures, Cornell University, Ithaca, New York, August 24-25, 1993.
5. Özbek, A., Shektman, I., Volovoi, V., Mueller, E., and Berdichevsky, V., "Statistical Mechanics of Beam Vibrations," presented at the 114th ASME Winter Annual Meeting, New Orleans, LA, November 29-December 3, 1993.

## References

- [1] Fermi, E., Pasta, J., and Ulam, S., "Studies of Nonlinear Problems," Los Alamos Scientific Laboratory, Report LA-1540, 1955
- [2] Arnold, V. I., Kozlov, V. V., and Neustadt, A. I., "Mathematical Aspects of Classical and Celestial Mechanics," Springer-Verlag, Berlin, 1987

- [3] Bocchiery, P., Scotti, A., Bearzi, B., and Loinger, A., "Anharmonic Chain with Lennard-Jones Interaction," *Physical Review A*, v. 2, 1970, pp. 2013-2019
- [4] Galgani, I., and Scotti, A., "Recent Progress in Classical Nonlinear Dynamics," *Revisita del Nuovo Cimento*, v. 2, 1972, 189-209
- [5] Chirikov, B., Izrailev, F., and Tayursky, V., "Numerical Experiments on the Stochastic Behavior of Dynamical Systems with a few Degrees of Freedom," *Computer Physics Communications*, 5, 1973, pp 11-16
- [6] Thirumalai, D., and Mountain, R. D., "Probes of Equipartition in Nonlinear Hamiltonian Systems," *J. Stat. Physics*, V. 57, 1989, pp. 789-801
- [7] Scotti, A., and Zanzucchi, F., "Permanence of Stochasticity Thresholds in KAM Systems," *Physical Review A* (to appear)
- [8] Berdichevsky, V., Özbek, A., Shekhtman, I., "Statistical Mechanics of Longitudinal Vibrations of Beams" (in preparation).
- [9] Berdichevsky, V., "Thermodynamics of Chaos," Pitman-Longman, 1994 (to appear).
- [10] Berdichevsky, V. "A Connection Between Thermodynamical Entropy and Probability," *Journal of Applied Mathematics and Mechanics* (PMM), vol. 52, No. 35, 1988, pp. 738-746.
- [11] Berdichevsky, V., and von Alberti, M., "Statistical Mechanics of Henon-Heliles Oscillators," *Physical Review A*, vol. 44, No. 8, pp 858-865, 1991
- [12] Berdichevsky, V., "Reciprocal Relations in Nonlinear Vibrations," *International Journal of Engineering Science*, Vol. 31, No. 8. pp. 1215-1218, 1993
- [13] Berdichevsky, V., Özbek, A., Kim, W. W., "Thermodynamics of Duffing's Oscillator," *Journal of Applied Mechanics* (to appear)
- [14] Berdichevsky, V., Kim, W. W., Özbek, A., "Dynamical Potential for Nonlinear Vibrations of a Cantilever Beam," *Journal of Sound and Vibrations*, (to appear)

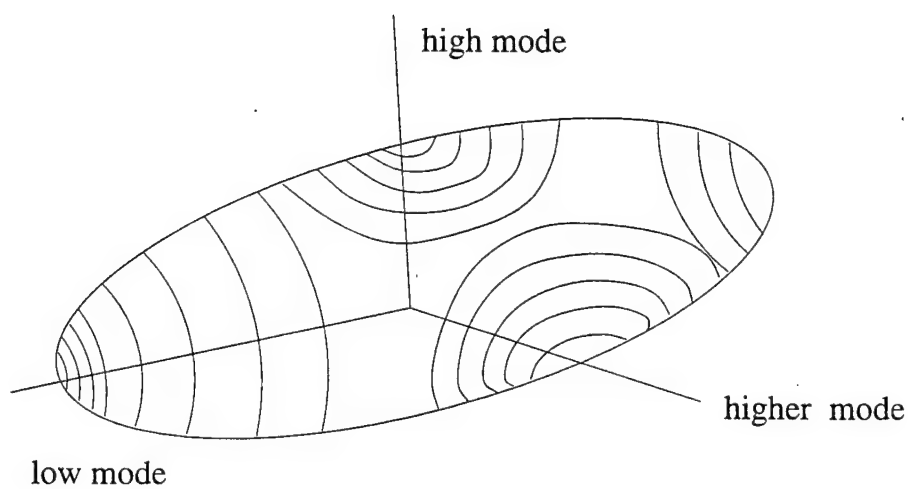


Figure 11: Sketch of energy surface for excitation less than  $E_c$

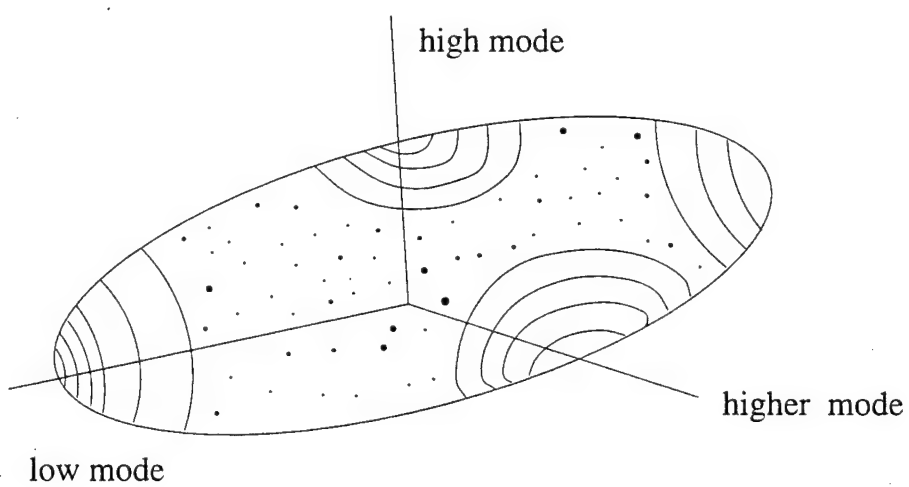


Figure 12: Sketch of energy surface for excitation less than  $E_c$



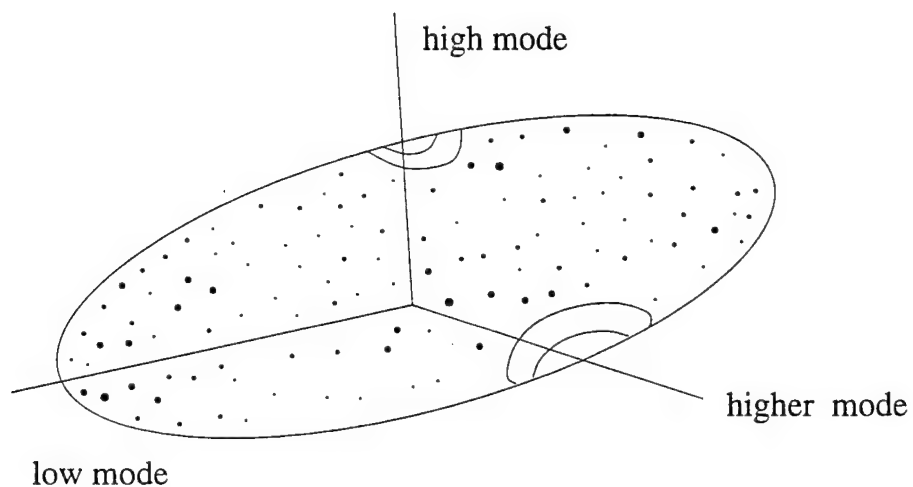


Figure 13: Sketch of energy surface for excitation greater than  $E_c$

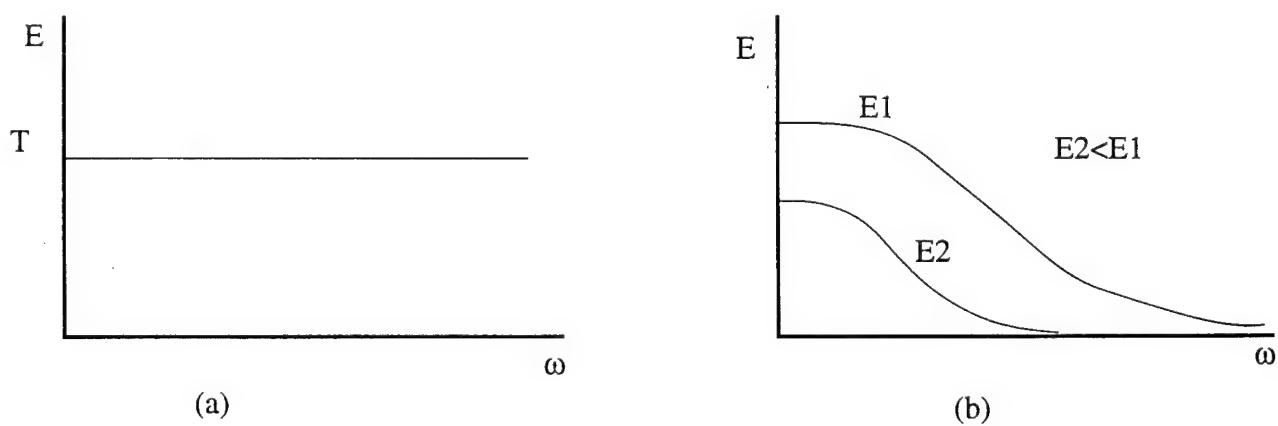


Figure 14: Energy Spectra: (a) Equipartition Holds, (b) Simulated  $E_c < \text{Total Energy}$

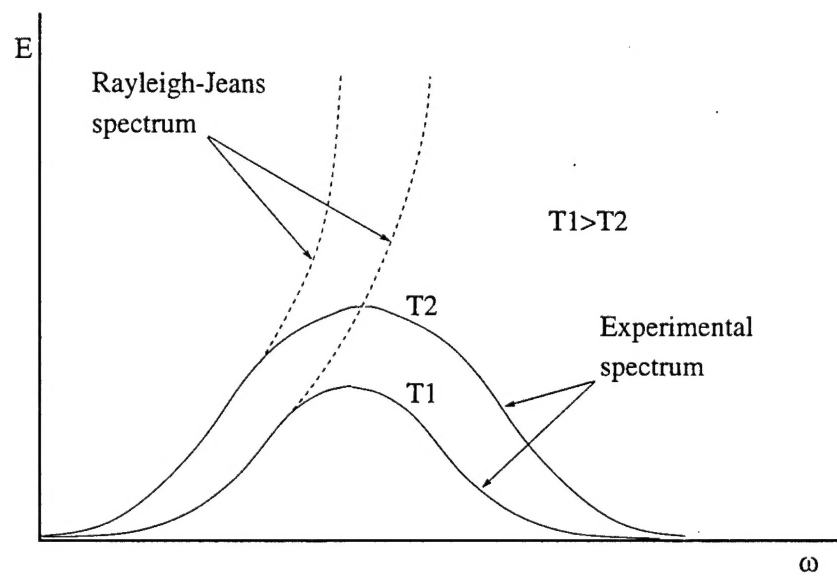


Figure 15: 3-D Energy Spectrum

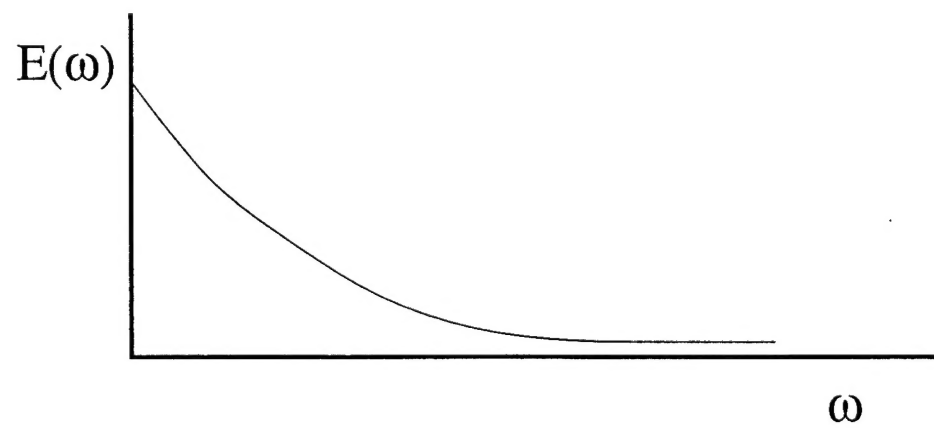


Figure 16: Plank's Spectrum

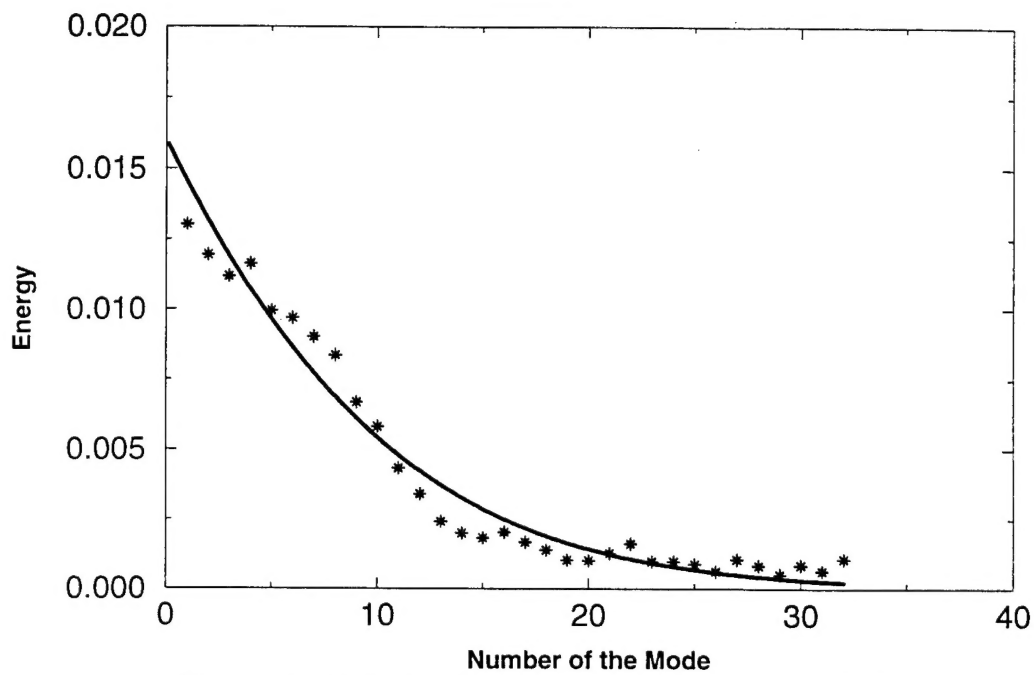


Figure 17: Calculated Energy Spectrum versus Plank's Spectrum

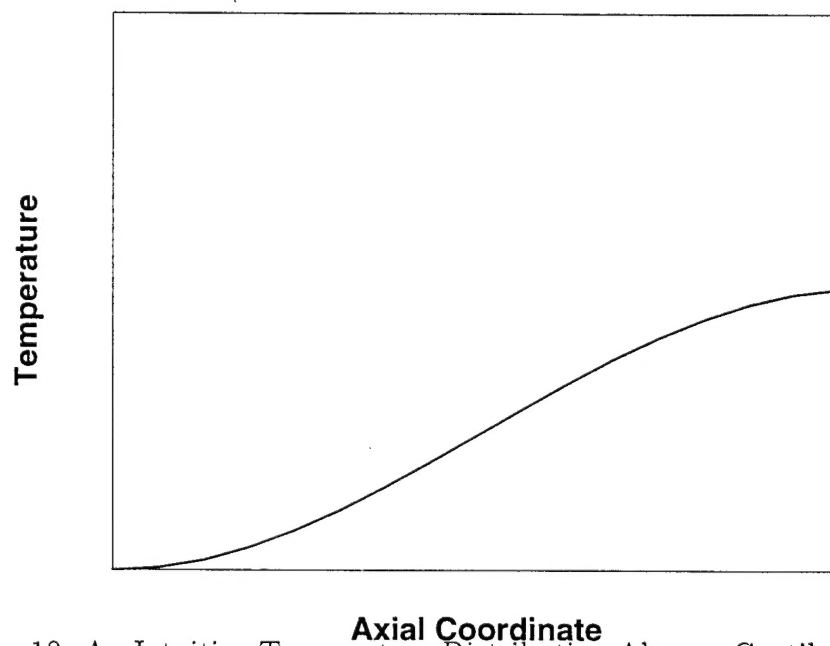


Figure 18: An Intuitive Temperature Distribution Along a Cantilever Beam

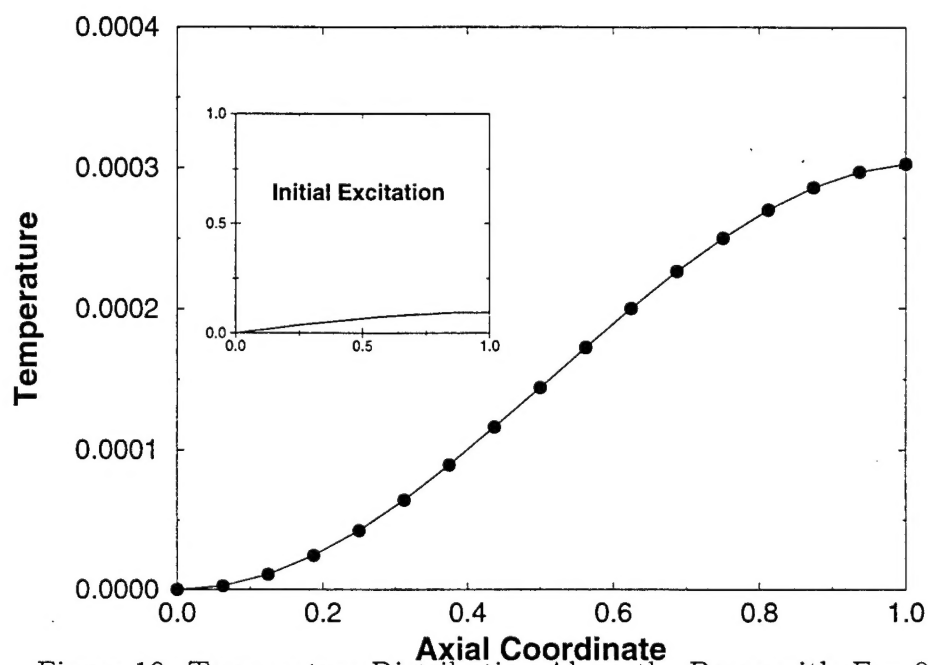


Figure 19: Temperature Distribution Along the Beam with  $E = 0.005$

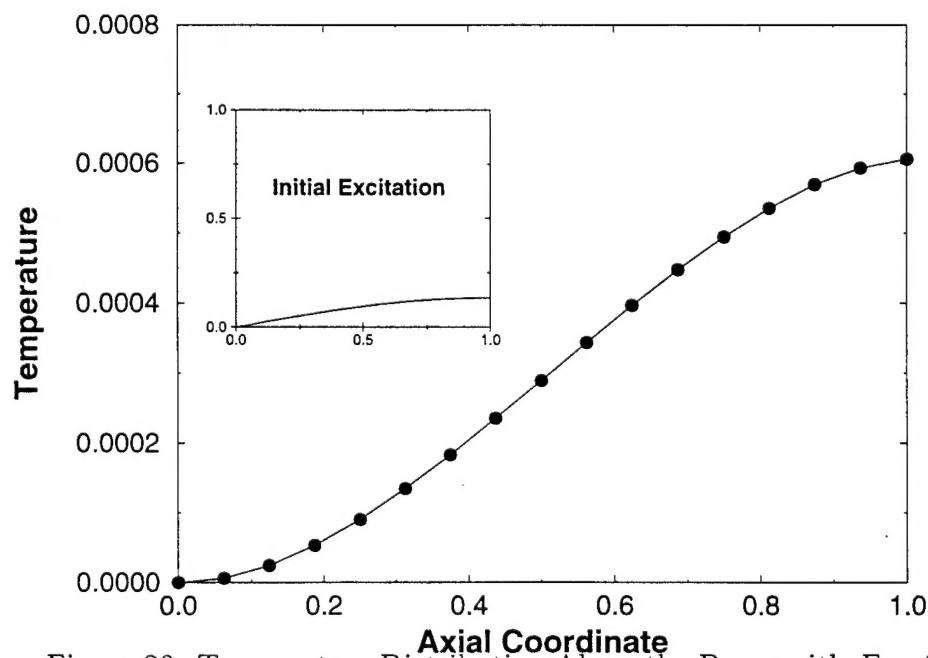
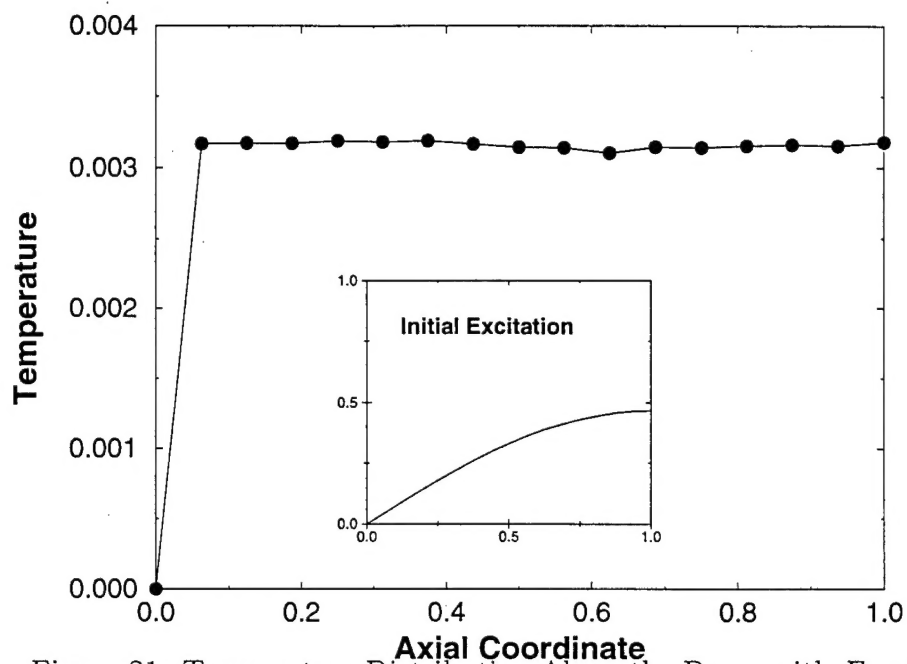
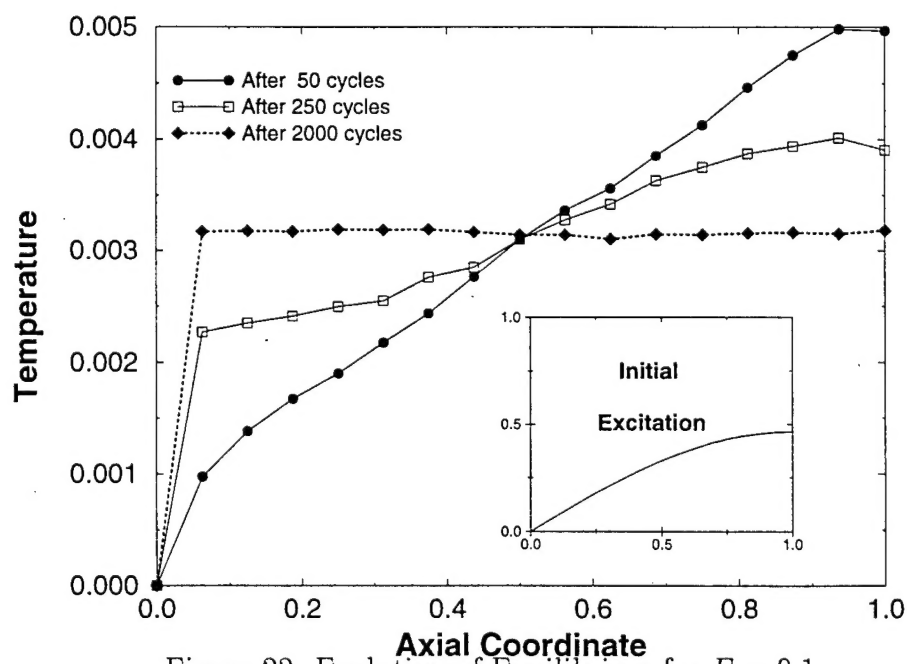


Figure 20: Temperature Distribution Along the Beam with  $E = 0.01$

Figure 21: Temperature Distribution Along the Beam with  $E = 0.1$ Figure 22: Evolution of Equilibrium for  $E = 0.1$